

ELEMENTAL ABUNDANCES IN STELLAR CORONAE WITH XMM-NEWTON

M. Audard and M. Güdel

Paul Scherrer Institut, Würenlingen and Villigen, 5232 Villigen PSI, Switzerland

ABSTRACT

The XMM-Newton Reflection Grating Spectrometer Team has obtained observations of a large number of coronal sources of various activity levels, ages, and spectral types. In particular, X-ray bright RS CVn binary systems display saturated coronal emission with spectral lines characteristic of hot (10-30 MK) plasma. Furthermore, we have obtained XMM-Newton data from young solar analogs both within and outside the X-ray saturation regime. We have simultaneously analyzed the EPIC MOS and RGS data from these objects and have obtained coronal abundances of various elements (e.g., C, N, O, Ne, Mg, Si, Fe). We show that there is evidence for a transition from an Inverse First Ionization Potential (FIP) effect in most active stars to a “normal” solar-like FIP effect in less active stars. We discuss this result with regard to photospheric abundances.

Key words: Missions: XMM-Newton – stars: abundances – stars: coronae

1. INTRODUCTION

High-resolution X-ray spectra of stellar coronae obtained by *XMM-Newton* and *Chandra* now allow us to study in detail the rich forest of X-ray lines emitted by elements abundant in stellar coronae, such as C, N, O, Ne, Mg, Si, S, Ar, Ca, Fe, and Ni. In the past, stellar coronal abundances have frequently been determined using the moderate spectral resolution of CCD spectra from *ASCA* (e.g., Drake 1996; Güdel et al. 1999) or from the low sensitivity spectrometers onboard *EUVE* (e.g., Drake et al. 1995; Laming et al. 1996; Schmitt et al. 1996; Drake et al. 1997). The abundance pattern in stellar coronae is complementary to the abundance pattern in the Sun: the solar corona, the solar wind, and solar energetic particles (and probably also galactic cosmic rays) display a so-called “First Ionization Potential” (FIP) effect, for which abundances of low-FIP (< 10 eV) elements are enhanced relative to their respective photospheric abundances, while the abundances of high-FIP (> 10 eV) elements are photospheric (Feldman 1992, see also Meyer 1985). Stellar coronal observations however often showed a deficiency of metals relative to the solar photospheric abundances (Schmitt et al.

1996). *EUVE* spectra either indicated the absence of any FIP-related bias (Drake et al. 1995), or a solar-like FIP effect (Drake et al. 1997) in inactive stellar coronae. The new X-ray observatories *XMM-Newton* and *Chandra* combine the high spectral resolution with moderate effective areas to routinely obtain data allowing to measure the abundances in stellar coronae.

Recently, Brinkman et al. (2001) showed a trend towards enhanced high-FIP elemental abundances, while low-FIP abundances are depleted; this effect was dubbed the “Inverse FIP” (IFIP) effect. Other active stars showed a similar trend (Güdel et al. 2001a; Güdel et al. 2001b), except the intermediately active Capella (Audard et al. 2001a). Note however that stellar coronal abundances have often been normalized to the *solar* photospheric abundances, while they should better be normalized to the *stellar* photospheric abundances. The latter are difficult to measure. Nevertheless, for some stars, photospheric abundances are known. The uncertainty introduced by photospheric abundances can then be removed. We will show that there is a transition from an IFIP to a normal FIP effect in the long-term evolution of the coronae from active to inactive solar analogs. We will use data of bright active RS CVn binary systems to complement the study as well. Finally, the variation of stellar coronal abundances during flares will be discussed.

2. OBSERVATIONS AND DATA ANALYSIS

XMM-Newton observed several coronal sources as part of the RGS stellar Guaranteed Time Program. Observations of active bright RS CVn binary systems (e.g., HR1099, Capella, UX Ari, λ And) provided excellent high-resolution RGS spectra. The solar past has also been probed with observations of young solar analogs of different ages and activity levels (e.g., AB Dor, EK Dra, π^1 UMa, χ^1 Ori). The RGS1, RGS2, and EPIC MOS2 spectra have been simultaneously fitted (except for Capella where there are no EPIC data available) in XSPEC 11.0.1aj (Arnaud 1996) using the *vappec* model (APEC code with variable abundances). Because of the inaccuracy and incompleteness of atomic data for non-Fe L-shell transitions, significant parts of the RGS spectra had to be discarded above 20 Å. Furthermore, some Fe L-shell lines with inaccurate atomic data were not fitted. For additional information

on the data analysis, we refer to Audard et al. (2002) and Güdel et al. (2002).

3. RESULTS

3.1. CORONAL ABUNDANCES OF ACTIVE STARS

The RGS spectra of four RS CVn-type systems shown in Figure 1 display bright H-like and He-like emission lines (mostly from C, N, O, Ne, Mg, Si) and numerous Fe L-shell lines. Although the overall spectral features are similar in HR 1099, UX Ari, and λ And, there are differences in terms of line intensities or ratios. This can suggest differences in the emission measure distributions, or in the elemental composition in their coronae. A hint pointing toward the latter interpretation comes from the different ratios of the Fe XVII (at 15Å) and Ne IX lines, which have similar maximum formation temperatures. The line ratio in Capella definitely points toward an abundance effect, with a high Fe/Ne ratio. We have performed fits (see §2) to the data and modeled the X-ray spectra. Coronal abundances (normalized to the oxygen abundance to remove the uncertainty that might be introduced by the determination of the underlying continuum) relative to the solar photospheric abundances are shown in Fig. 2 as a function of the first ionization potential of the element. A similar trend (IFIP effect) as found by Brinkman et al. (2001) is seen in UX Ari, with low-FIP elements depleted relatively to the high-FIP elements, and confirmed in this new analysis of HR 1099. In contrast, the FIP bias in λ And is less clear. The absence of any FIP bias is suggested in the intermediately active binary Capella.

Since reliable determinations of *stellar* photospheric abundances in active stars are rare, we cannot normalize the derived coronal abundances by their photospheric counterparts. Hence, it is possible that the FIP bias observed in HR 1099 and UX Ari is simply a reflection of their photospheric composition. However, it is possible to use stars with known photospheric abundances to determine whether a FIP effect (or its inverse) exists in active stars. We have used spectra from solar analogs (Fig. 3) for which the photospheric composition is close to solar. These stars represent the Sun in its past and probe its activity in its infancy. While AB Dor is strictly speaking not a solar analog (spectral type K0), its activity is similar to that of a very active young Sun. Similarly to the RS CVn binary systems, the differences in the spectral features do not depend solely on the emission measure distribution, but also on intrinsic variations of coronal abundances. Spectral fits confirm that the coronal composition of our sample is different for each star. Figure 4 shows the coronal abundances as a function of the FIP, like in Fig. 2. The FIP bias appears to correlate with the activity level (or age): an IFIP effect is found in the most active star AB Dor, like in the most active RS CVn binaries, while the intermediately active EK Dra shows no pronounced bias. Finally, the oldest, less active stars π^1 UMa and χ^1 Ori

display a similar abundance bias, close to that observed in the Sun. Note that the transition in the FIP bias occurs for low-FIP elements while the high-FIP elements appear to have similar coronal abundances (normalized to oxygen) in all stars.

Based on the emission measure distributions obtained from multi-temperature fits, we have calculated a logarithmic average temperature and defined the latter as the average coronal temperature. While most inactive stars have temperatures between 4 and 6 MK, RS CVn binary systems display average quiescent temperatures around 10–20 MK. Previous analysis showed a correlation between the X-ray luminosity of solar analogs and their average coronal temperatures (Güdel et al. 1997). The average coronal temperature can therefore be considered to be an activity indicator. The abundances of low-FIP elements correlate with the coronal temperature. While they are depleted in the most active stars, a transition occurs with decreasing temperature, and their abundances drastically increase (relative to high-FIP elements). On the other side, the abundances of high-FIP elements stay constant. In Figure 5 we give examples for Fe and Ne, representing low-FIP elements and high-FIP elements, respectively. Note that this behavior is reproduced in other low-FIP elements (e.g., Mg, Si) and high-FIP elements (e.g., C, N).

3.2. CORONAL ABUNDANCE DURING FLARES

In the previous section, coronal abundances of active stars in *quiescence* have been reported to show a transition from under- to overabundant low-FIP elements with decreasing activity (or coronal temperature), while the high-FIP elemental abundances stay constant (relative to oxygen). However, previous data showed that the average metallicity Z or the Fe abundance can increase during large flares (e.g., Ottmann & Schmitt 1996). Güdel et al. (1999) obtained time-dependent measurements of several elemental abundances during a large flare in UX Ari with *ASCA*. The abundance of low-FIP elements increased more significantly than those of high-FIP elements. Recently, Audard et al. (2001b) found a similar behavior in the *XMM-Newton* data of a flare in HR 1099. We have redone the analysis of this flare using a more recent calibration. Figure 6 shows the Fe/O and Ne/O ratios versus the coronal temperature of HR 1099, before the flare (quiescence), during the flare rise, and at flare peak (no complete decay available). Consistently with our previous analysis (Audard et al. 2001b), we have found that the absolute Fe abundance increases during the rising part of the flare. In contrast, the absolute Ne abundance stays constant. Other low-FIP elements and high-FIP elements show similar respective behavior. Note, however, that the signal-to-noise ratio in the RGS time-dependent spectra did not allow us to better sample the flare event. Longlasting strong flares are needed to obtain high-quality spectra of a flare.

4. CONCLUSIONS

High-resolution X-ray spectra of magnetically active stars have been investigated with the Reflection Grating Spectrometers on board *XMM-Newton*. The high-energy data (> 1.5 keV) of the EPIC CCD spectra were used to better constrain the high-temperature part of the emission measure distributions and to profit from the presence of H-like and He-like transitions of Si, S, Ar, and Ca. It was found that the most active stars, such as the bright RS CVn binary systems, show a marked depletion of low-FIP elements (e.g., Fe, Mg, Si) relative to high-FIP elements (e.g., C, N, O, Ne), opposite to the FIP effect observed in the solar corona. This “inverse FIP” effect is however not observed in the intermediately active RS CVn binary Capella. Since their photospheric abundances are mostly unknown or not reliable, one can hypothesize that the observed FIP bias is simply a reflection of their photospheric composition.

To remove the uncertainty of surface abundances, we have analyzed high-resolution X-ray spectra of solar analogs of known photospheric composition (close to solar). These solar-like stars span a wider range of coronal activity (from inactive to active) and represent the evolution of the solar corona in time. We have found a transition from a depletion of low-FIP elements (relative to high-FIP elements) in the most active stars toward a marked enhancement of their abundances in the inactive stars. On the other hand, the abundances of high-FIP elements do not vary with the activity level (or coronal temperature), relative to O. The IFIP effect found in the active RS CVn binary systems fit well into this transition, under the assumption that their photospheric composition is also close to solar. Similarly, the solar FIP effect (enhancement of low-FIP elements by factors of 4–8) fits into this picture. However, although the scenario of correlating the activity level with the FIP bias is tempting, it may be too simplistic; indeed, such scenario does not explain the absence of any FIP bias in the corona of the old, inactive Procyon (Drake et al. 1995).

We have put forward first ideas to explain the inverse FIP effect seen in active stars: downward propagating electrons detected by their gyrosynchrotron emission in active stars could prevent chromospheric ions (mostly low-FIP elements) from escaping into the corona by building up a downward-pointing electric field (Güdel et al. 2002). As the density of high-energy electrons decreases with decreasing activity, the inverse FIP effect is quenched. During large flares, however, the high-energy electrons heat a significant portion of the chromosphere to bring up a near-photospheric mixture of elements into the corona, and this effect has indeed been observed (Güdel et al. 1999; Audard et al. 2001b). The new results by *XMM-Newton* and *Chandra* have opened a new field of research relevant to the physics of heating and dynamics of outer stellar atmospheres.

ACKNOWLEDGEMENTS

We acknowledge support from the Swiss National Science Foundation (grant 2100-049343). This work is based on observations obtained with XMM-Newton, an ESA science mission with instruments and contributions directly funded by ESA Member States and the USA (NASA).

REFERENCES

- Anders, E., & Grevesse, N. 1989, *Geochim. Cosmochim. Acta*, 53, 197
- Arnaud, K. A. 1996, in *ASP Conf. Ser. 101, Astronomical Data Analysis Software and Systems V*, ed. G. Jacoby & J. Barnes (San Francisco: ASP), 17
- Audard, M., Behar, E., Güdel, M., et al. 2001a, *A&A*, 365, L329
- Audard, M., Güdel, M., & Mewe, R. 2001b, *A&A*, 365, L318
- Audard, M., Güdel, M., et al. 2002, *A&A*, in preparation
- Brinkman, A. C., Behar, E., Güdel, M., et al. 2001, *A&A*, 365, L324
- Drake, J. J., Laming, J. M., & Widing, K. G. 1995, *ApJ*, 443, 393
- Drake, J. J., Laming, J. M., & Widing, K. G. 1997, *ApJ*, 478, 403
- Drake, S. A. 1996, in *Proceedings of the 6th Annual October Astrophysics Conference in College Park*, eds. S. S. Holt & G. Sonneborn, (San Francisco: ASP), 215
- Feldman, U. 1992, *Physica Scripta*, 46, 202
- Grevesse, N., & Sauval, A. J. 1999, *A&A*, 347, 348
- Güdel, M., Audard, M., Briggs, K., et al. 2001a, *A&A*, 365, L336
- Güdel, M., Audard, M., Magee, H., et al. 2001b, *A&A*, 365, L344
- Güdel, M., Audard, M., Sres, A., Wehrli, R., & Mewe, R. 2002, *ApJ*, submitted
- Güdel, M., Guinan, E. F., & Skinner, S. L. 1997, *ApJ*, 483, 947
- Güdel, M., Linsky, J. L., Brown, A., & Nagase, F. 1999, *ApJ*, 511, 405
- Laming, J. M., Drake, J. J., & Widing, K. G. 1996, *ApJ*, 462, 948
- Meyer, J.-P. 1985, *ApJS*, 57, 173
- Ottmann, R., & Schmitt, J. H. M. M. 1996, *A&A*, 307, 813
- Schmitt, J. H. M. M., Stern, R. A., Drake, J. J., & Kürster, M. 1996, *ApJ*, 464, 898

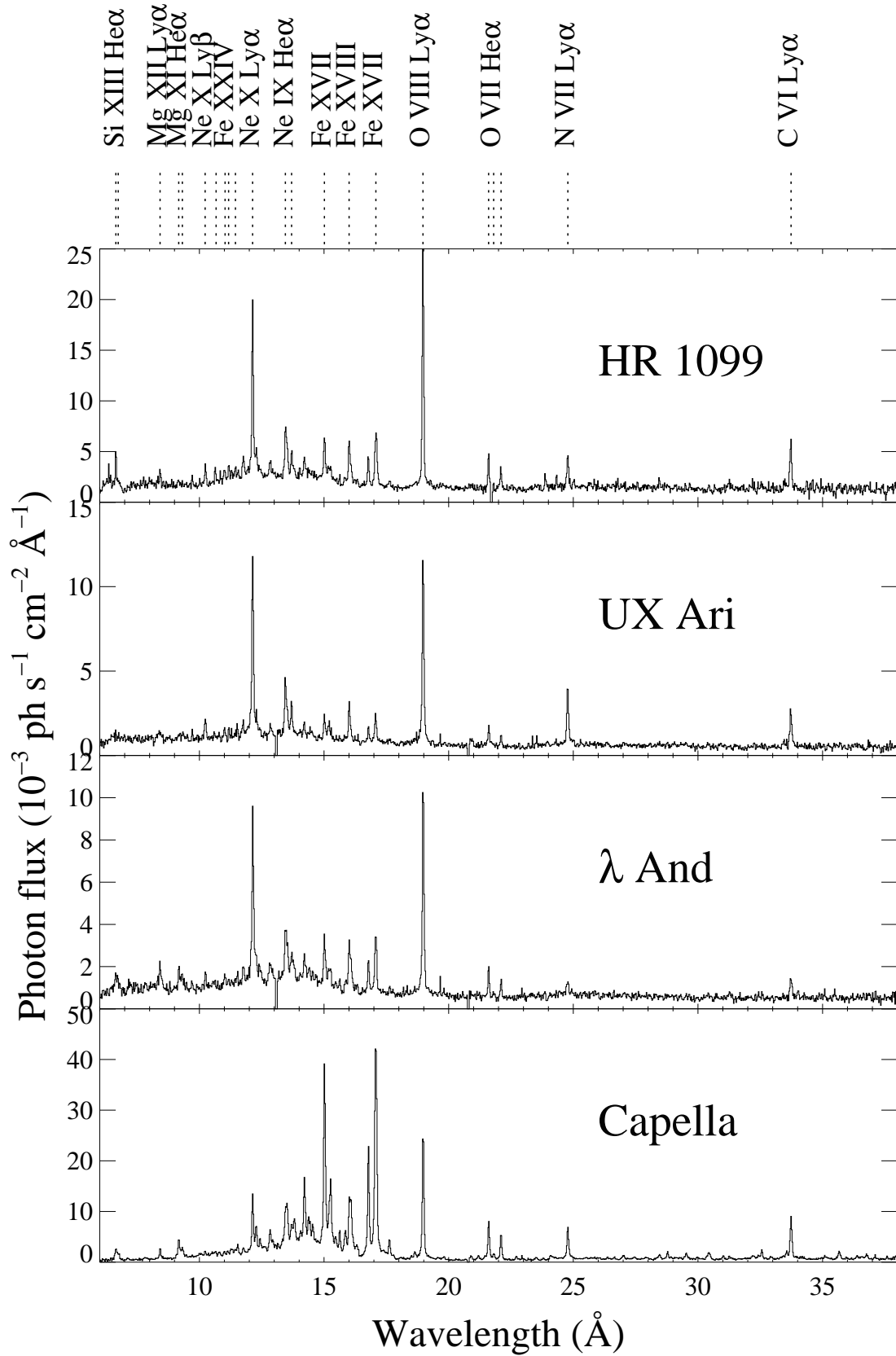


Figure 1. RGS spectra of bright active RS CVn binary systems. The sources have been ordered with decreasing activity levels (or average coronal temperature) from top to bottom. Major emission lines have been labeled.

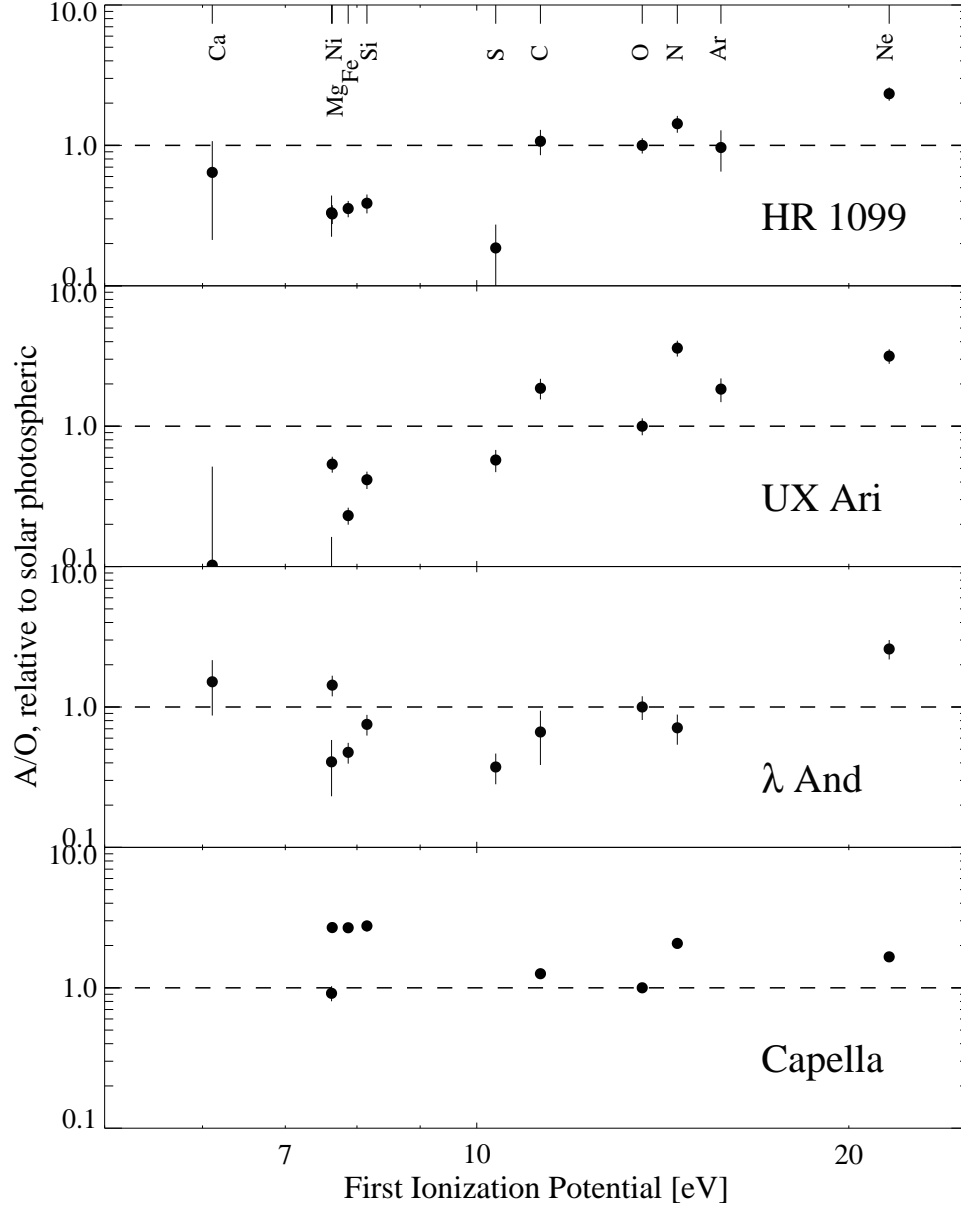


Figure 2. Coronal abundance normalized to oxygen in RS CVn binaries as a function of the First Ionization Potential. Solar photospheric abundances from Anders & Grevesse (1989) were used, except for Fe (Grevesse & Sauval 1999).

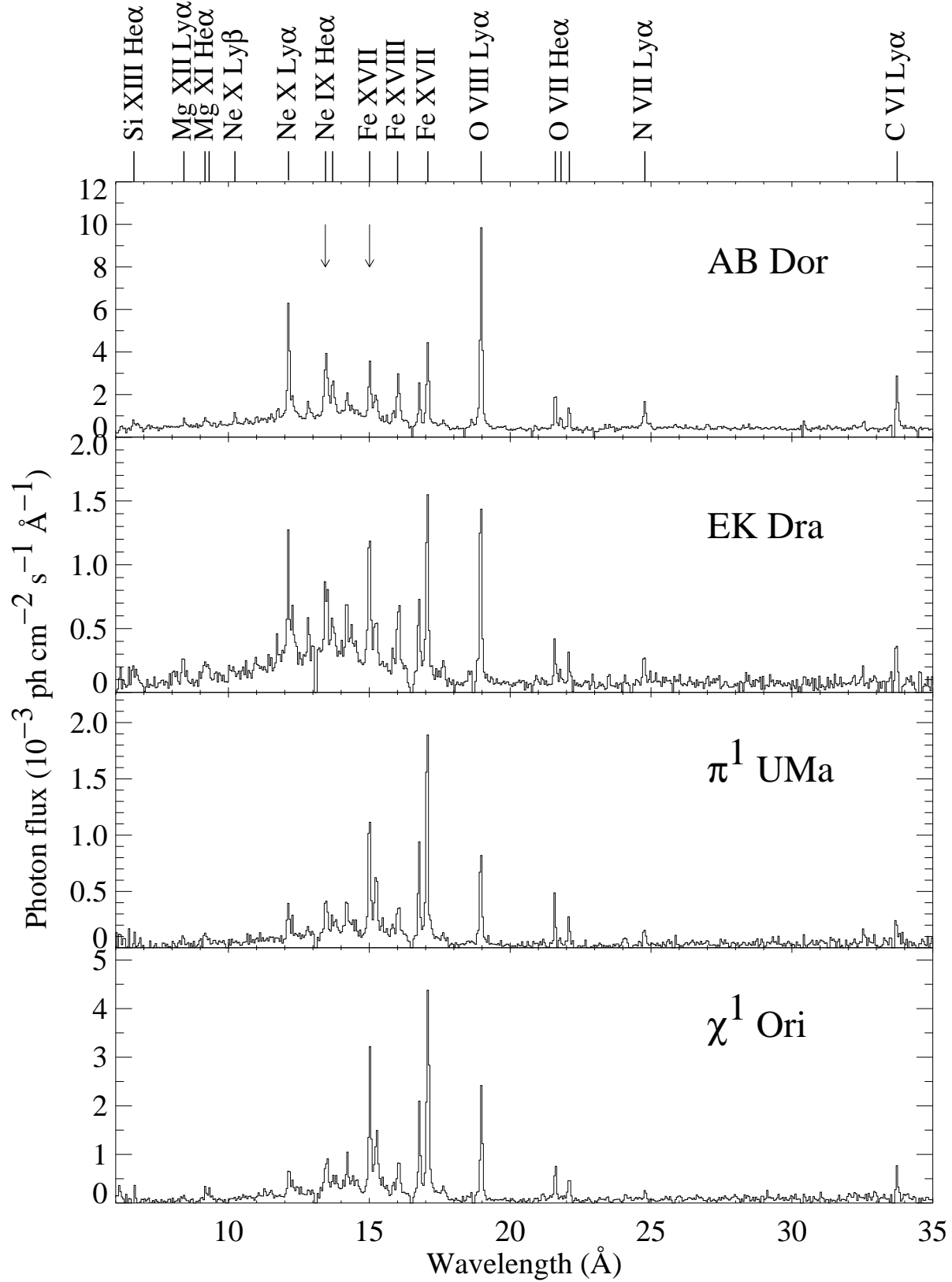


Figure 3. RGS spectra of solar analogs. Their order is set similarly to Fig. 1. The arrows designate lines with similar maximum formation temperature; hence different line ratios of the Fe XVII line at 15 Å and the Ne IX line suggest differences in coronal abundances in each star.

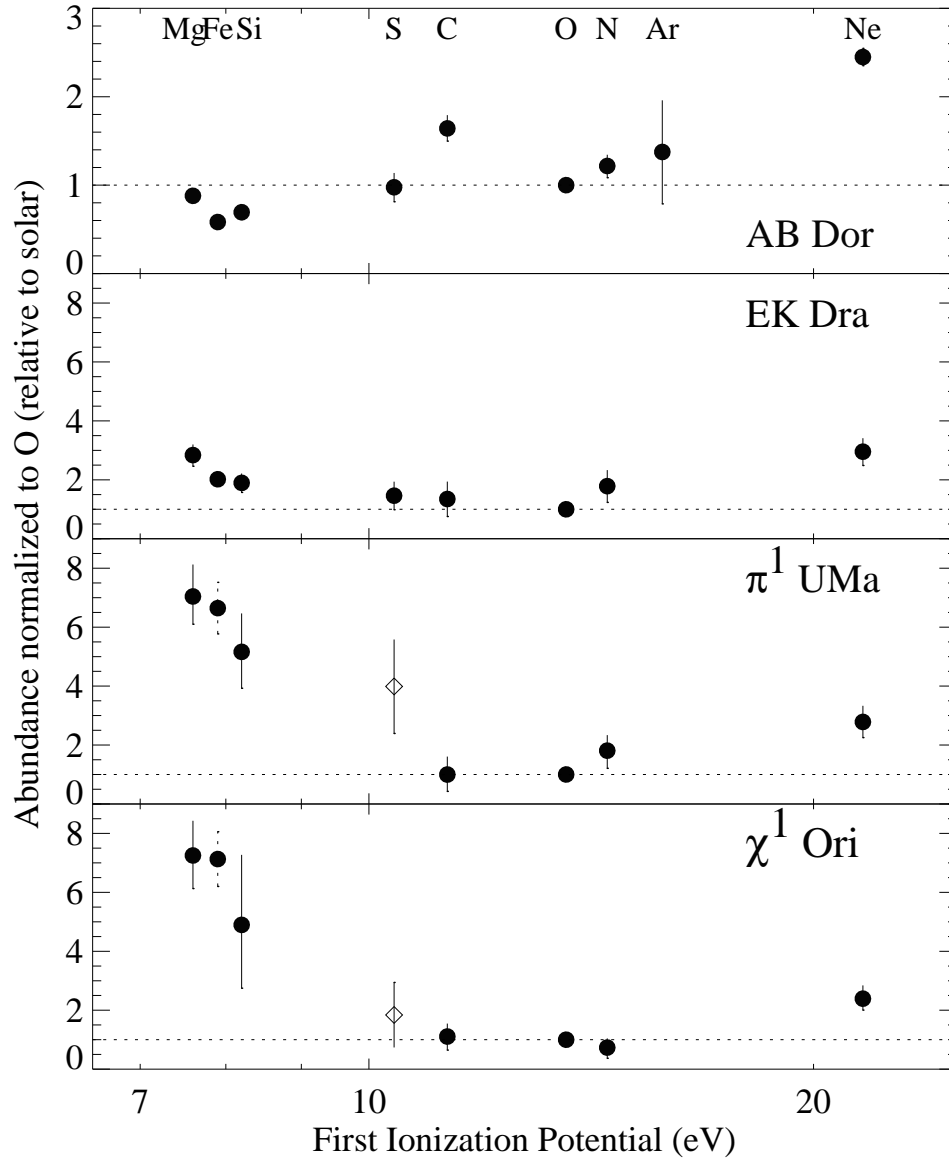


Figure 4. Coronal abundance normalized to oxygen in solar analogs as a function of the First Ionization Potential. Note that the activity level decreases (their age increases) from top to bottom. Similar photospheric abundances have been taken as in Fig. 2.

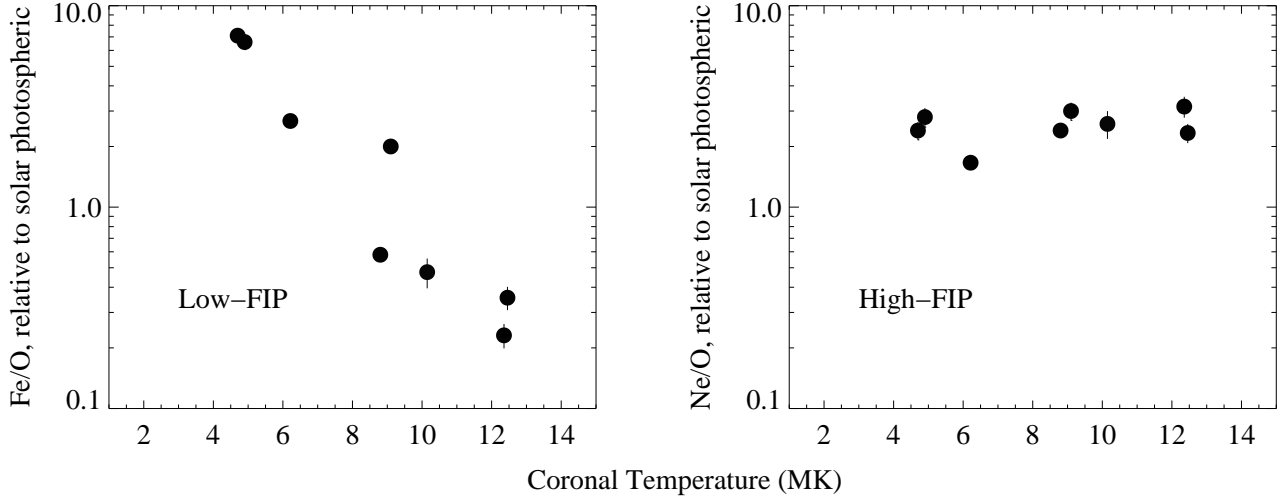


Figure 5. Coronal abundances (normalized to O) as a function of the average coronal temperatures, for Fe (low-FIP; left) and Ne (high-FIP; right). The data include solar analogs and RS CVn binaries.

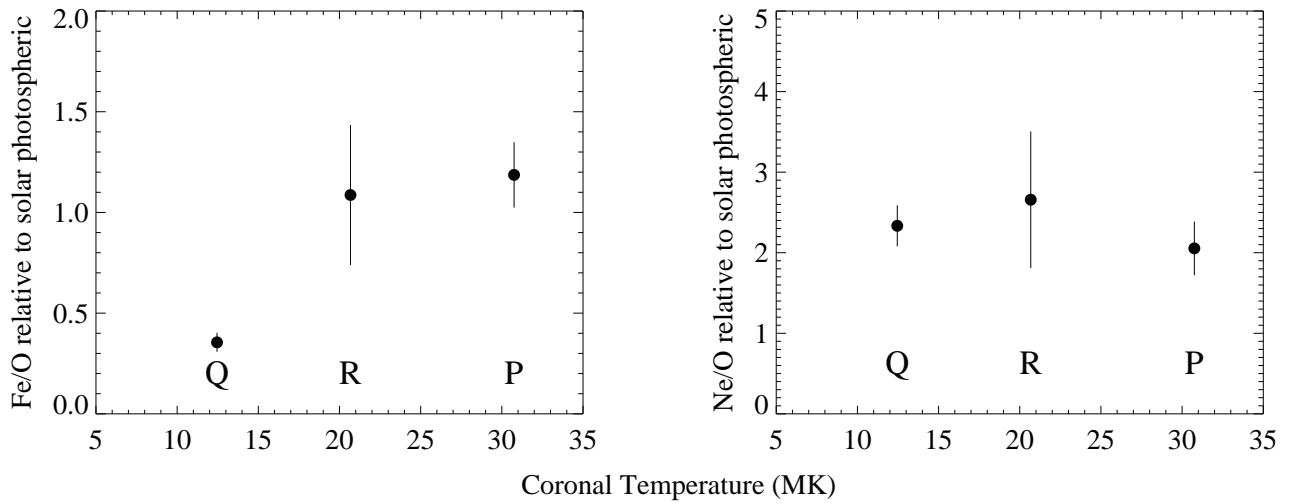


Figure 6. Coronal abundances (normalized to O) as a function of the average coronal temperature during a large flare in HR 1099. Left panel gives Fe/O ratios, while the right panel gives Ne/O ratios. 'Q' stands for quiescent, 'R' for flare rise, and 'P' for flare peak.